HHS Public Access

Author manuscript

Nature. Author manuscript; available in PMC 2012 December 07.

Published in final edited form as:

Nature. ; 486(7401): 122–125. doi:10.1038/nature11033.

alpha2delta expression sets presynaptic calcium channel abundance and release probability

Michael B. Hoppa[1], **Beatrice Lana**[2], **Wojciech Margas**[2], **Annette C. Dolphin**[2], and **Timothy A. Ryan**[1]

[1]Department of Biochemistry, Weill Cornell Medical College

[2]Department of Neuroscience, Physiology and Pharmacology, University College London

Synaptic neurotransmitter release is driven by Ca^{2+} influx through active zone voltage-gated calcium channels (VGCCs)[1,2]. Control of active zone VGCC abundance and function remains poorly understood. We show that a trafficking step likely sets synaptic VGCC levels as overexpression of the pore-forming $\alpha 1_A$ fails to change synaptic VGCC abundance or function. α2δs are a family of GPI-anchored VGCC-associated subunits[3], which in addition to being the target of the potent neuropathic analgesics gabapentin and pregabalin (α2δ-1, α2δ-2)[4,5], were also identified in a forward genetic screen for pain genes (α2δ-3)[6]. We show that these proteins confer powerful modulation of presynaptic function through two distinct molecular mechanisms. α2δ subunits set synaptic VGCC abundance, as predicted from their chaperone-like function when expressed in non-neuronal cells[3,7]. Secondarily, α2δs configure synaptic VGCCs to drive exocytosis through an extracellular metal ion-dependent adhesion site (MIDAS), a conserved set of amino acids within α2δ's predicted von Willebrand A (VWA) domain. Expression of α2δ with an intact MIDAS motif leads to an 80% increase in release probability, while simultaneously protecting exocytosis from blockade by an intracellular Ca^{2+} chelator. α2δs harboring MIDAS site mutations still drive synaptic accumulation of VGCCs however, they no longer change release probability or sensitivity to intracellular Ca^{2+} chelators. Our data reveal dual functionality of these clinically important VGCC subunits, allowing synapses to make more efficient use of Ca^{2+} entry to drive neurotransmitter release.

VGCCs are composed of pore-forming α1 and auxiliary β and α2δ subunits[8,9]. In central synapses neurotransmitter release is generally driven by P/Q-type ($\alpha 1_A$) and/or N-type ($\alpha 1_B$)10 VGCCs. Based on the failure of $\alpha 1_A$ overexpression to increase synaptic strength, it had been suggested that VGCCs functionally coupled to presynaptic release machinery is

Correspondence and requests for materials should be addressed to taryan@med.cornell.edu.

Supplementary Information is linked to the online version of the paper at www.nature.com/nature

Author Contributions: MHB performed opto-physiological experiments, BL and WM performed electrophysiological experiments, AD, BL & WM designed electrophysiological experiments, MHB, AD & TAR designed all other experiments, MHB, AD & TAR wrote the manuscript.

The authors declare that they have no competing financial interests.

limited by a fixed number of available "slots" where channels can insert into the synaptic membrane[11]. We examined the existence of such a bottleneck by expressing eGFP-$\alpha 1_A$12 together with a reporter of presynaptic exocytosis (vGlut1 with a luminal tag mOrange2, vGmOr2) and carried out retrospective immunocytochemistry to probe the abundance of $\alpha 1_A$ in transfected compared to control neurons. eGFP-$\alpha 1_A$ correctly trafficked to nerve terminals as it co-localized well with the vesicle-targeted reporter (Fig. 1a). In order to ensure eGFP-$\alpha 1_A$ functionally integrated with endogenous channels to drive neurotransmitter release we introduced a point mutation (E1656K), rendering this channel insensitive to the antagonist ω-agatoxin IVA[13]. Under control conditions a combination of ω-agatoxin IVA and the $\alpha 1_B$ inhibitor ω-conotoxin GVIA completely blocked vGmOr2 responses to action potential (AP) firing, however in the presence of eGFP-$\alpha 1_A^{E1656K}$ a significant fraction of the response remains (Fig 1b). Measurements of single AP responses showed that expression of this exogenous $\alpha 1_A$ did not alter exocytosis efficiency compared to controls (Fig. 1c–d), consistent with the "slot" hypothesis[11]. However, retrospective immunocytochemistry using an anti-$\alpha 1_A$ antibody whose specificity was verified using shRNA-mediated $\alpha 1_A$ knockdown (Fig. S1) showed that transfected and control nerve terminals had similar immunoreactivity (Fig. 1e–f) while at the cell soma it had doubled (Fig S2). These results demonstrate that synaptic VGCC abundance is likely limited by trafficking from the cell soma and failure to increase synaptic performance does not result from a fixed number of active zone insertion sites. α2δ and β auxiliary VGCC subunits are both strong candidates for modulating such trafficking as they control functional expression of α1 subunits when co-expressed in non-neuronal cells[14,15]. We coexpressed individual auxiliary subunits with the reporter vGlut1-pHluorin (vGpH) in neurons and carried out measurements of exocytosis and immunocytochemistry as described above. These experiments demonstrated that expression of either α2δ-1 or β4 subunits led to a significant increase (~3-fold, $p>0.05$) in synaptic abundance of $\alpha 1_A$ (Fig. 1e–f). Similar results were obtained with overexpression of α2δ-2 (Fig. 1f). Furthermore, introduction of shRNA targeting α2δ-1 caused depletion of $\alpha 1_A$ at nerve terminals (Fig. 1e–f, Figure S3), while leaving the somatic concentration unaltered (data not shown). These results demonstrate that synaptic $\alpha 1_A$ levels are titrated by expression of auxiliary VGCC subunits.

To examine whether changes in VGCC accumulation alters synaptic release properties, we measured single AP-stimulated exocytosis in neurons with altered VGCC levels. Overexpression and depletion of α2δ–1 led to much larger and much smaller single AP responses respectively compared to control (Fig. 2a). Similar increases in exocytosis were observed following expression of all three isoforms of α2δ tested (Fig. 2b). In contrast, expression of β4 did not change exocytosis, despite the synaptic accumulation of $\alpha 1_A$ (Fig. 2b). Quantitative estimates of α2δ-1 synaptic expression levels suggest a stoichiometric relationship between α2δ and $\alpha 1_A$ (Fig. S4). These results demonstrate that increasing VGCC abundance does not necessarily lead to increased function, and identify α2δ expression as a key rate-limiting parameter in determining presynaptic function.

Measurements of presynaptic strength can be parsed into two biophysical parameters: the number of vesicles available for rapid release upon stimulation, known as the readily-releasable pool (RRP) and the probability that a vesicle in the RRP will undergo fusion with a single AP stimulus (Pv)[16]. We recently developed a rapid depletion protocol to measure

RRP sizes using optical methods[17]. High frequency stimulation leads to rapid exhaustion of exocytosis in the first 8–15 APs. The fraction of the total pool corresponding to this rapid depletion phase is taken as the RRP[17] (Fig. 2c–d). The RRP size in neurons overexpressing α2δ was no different than controls (Fig. 2e). Thus α2δ overexpression changes Pv (Fig. 2f).

α2δ-driven increases in Pv might arise from increasing total Ca^{2+} influx (from changes in VGCC gating and/or surface abundance) and/or changing VGCC proximity to release sites [18]. To examine this question, we measured intracellular [Ca^{2+}] at synaptic boutons in response to single APs using the fast fluorescent indicator of Ca^{2+}, Fluo5F-AM, visualized by expression of VAMP-mCherry (VAMPmCh; Fig. 3a left panel) with or without α2δ. Single APs resulted in robust Ca^{2+} signals (Fig. 3a right panel) that peaked within 1 ms. but were reduced by ~40% in synapses overexpressing α2δ isoforms compared to controls (Fig. 3b–c). We verified that the peak signal was not dominated by Ca^{2+} clearance mechanisms (e.g. endogenous buffers or extrusion) in experiments where the signal decay was set by high concentrations of intracellular EGTA. This treatment led to a ~50% decrease in peak signal and a decay time of ~10 ms in controls as well as α2δ overexpressing synapses. Measurements of Ca^{2+} signals using a genetically encoded Ca^{2+} indicator GCaMP3[19], co-expressed with or without α2δ-1 gave very similar results (Fig. S5). This reduction in Ca^{2+} was surprising given that α2δ overexpression increases the total number of synaptic VGCCs (surface and intracellular) suggesting that α2δ might additionally control Ca^{2+} influx. Measurements of somatic AP waveforms revealed that α2δ expression led to a ~30% decrease in AP duration (Fig. S6), providing a possible explanation for the drop in synaptic Ca^{2+} entry. Given that exocytosis at nerve terminals is steeply dependent on Ca^{2+} influx[20], the proximity of sites of Ca^{2+} influx to sites of exocytosis can, in principle, have a powerful influence over neurotransmitter release[2]. The increase in Pv with a commensurate decrease in Ca^{2+} influx strongly suggests that overexpression of α2δ subunits results in a tighter spatial relationship between sites of Ca^{2+} entry and exocytosis. We tested this hypothesis by measuring the sensitivity of exocytosis to the presence of a Ca^{2+} chelator (EGTA-AM). The chelator's efficiency in reducing exocytosis depends on its ability to buffer Ca^{2+} before it binds the calcium-sensor for exocytosis following VGCC opening, a process determined by chelator concentration and Ca^{2+} binding kinetics[21]. We chose incubation conditions for EGTA-AM that led to a ~50% reduction in single AP exocytosis responses, compared to the pre-EGTA condition in control neurons (Fig. 3d). In neurons transfected with α2δ however, EGTA application led to much smaller decreases in exocytosis (Fig. 3e) indicating that in conditions of α2δ overexpression Ca^{2+} must bind the calcium sensor more rapidly than in control conditions. Therefore the Ca^{2+} sensor controlling exocytosis is experiencing higher levels of Ca^{2+} influx even though overall synaptic Ca^{2+} transients are reduced. Single AP-driven Ca^{2+} influx remained equally sensitive to ω-conotoxin GVIA following α2δ overexpression indicating this condition did not lead to a significant shift in VGCC type at nerve terminals (Fig. S7).

The finding that α2δ subunits form GPI-anchored proteins[3] implies that their ability to change VGCC-exocytosis coupling is likely conveyed through an extracellular interaction. One possible candidate for exerting such influence lies in the highly-conserved VWA domain within α2δ[22]. A characteristic feature of this domain is its ability to interact with adhesion proteins via the MIDAS motif by sharing coordination of a divalent cation[23–25]. To

examine the role of α2δ's MIDAS motif we mutated three of five conserved key metal coordinating residues within the MIDAS motif to alanine[22] and expressed the mutant protein (α2δ-1 MIDAS^{AAA}) in neurons together with functional reporters. α2δ-1 MIDAS^{AAA} was similar to wild type α2δ-1 in its ability to drive $\alpha1_A$ accumulation at synapses (Fig. 4a). However, measurements of exocytosis from α2δ-1 MIDAS-mutants showed no enhancement of Pv (Fig. 4b), normal Ca^{2+} influx (Fig. 4c) and normal sensitivity to EGTA block of exocytosis (Fig. 4d). Furthermore α2δ-2 MIDAS^{AAA}, unlike intact α2δ-2, was unable to rescue the decrease in exocytosis resulting from shRNA-mediated α2δ-1 depletion (Fig. 4e,f). These data are consistent with the ability of this mutation to block enhancement of Ca^{2+} currents when expressed in heterologous systems[22] (Fig. S8), but show that they do not prevent endogenous α2δ from functioning. Taken together, these results demonstrate that α2δ exerts its powerful control of synaptic VGCC function through at least two separate molecular mechanisms: a forward trafficking-step from cell body to presynaptic terminal that is independent of MIDAS motif integrity; and a local MIDAS-dependent interaction critical for proper VGCC function and coupling to exocytosis.

α2δ-1 and α2δ-2 are the targets of the analgesic gabapentin whose binding site lies in close proximity to the MIDAS site[26]. We found no significant impact of gabapentin application (30 min and >72 h) on Pv in either control or cells overexpressing α2δ-1 or -2 (results not shown) similar to previous findings in hippocampal neurons[27]. We also examined gabapentin's impact on VGCC trafficking to nerve terminals by incubating neurons with gabapentin from the time of transfection with eGFP-$\alpha1_A$. Analysis of the presynaptic abundance of this probe after 7 days showed that even though gabapentin appears to impact α2δ-2 trafficking in non-neuronal cells[28] it appears unable to impact VGCC trafficking or function in cultured hippocampal neurons (Fig. S9).

Our results reveal that α2δ subunits are potent modulators of synaptic transmission. They function through at least two distinct molecular mechanisms: a trafficking step from the cell soma and a local step at the presynaptic terminal allowing synapses to exhibit increased exocytosis with decreased Ca^{2+} influx. We speculate that increased presynaptic abundance of VGCCs results in increased abundance of active zone-VGCCs, and hence a higher density in the vicinity of release sites. This active zone accumulation depends on α2δ's VWA domain, presumably through interactions with extracellular active zone-specific proteins. The identity of the interaction partner(s) at present remains unknown however it is tempting to speculate that α2δs might recognize cues established in the correct juxtaposition of pre and postsynaptic membranes, consistent with synaptic defects observed in *Drosophila* α2δ-3 mutants[29]. Additionally this model requires that α2δ interact with a partner resulting in AP shortening to limit total calcium entry. As the MIDAS motif is well conserved throughout the α2δ family, identification of α2δ interaction partners in specific neuronal circuits could provide novel targets in the development of future therapeutics, given the potency that these subunits show in controlling synapse function.

Methods

Hippocampal CA3–CA1 regions were dissected from 1- to 3-day-old Sprague Dawley rats, dissociated, plated and transfected as previously described[30]. Live-cell images were

acquired with an Andor iXon$^+$ (model #DU-897E-BV) camera. A solid-state diode pumped 488 nm (vGpH and MgG imaging) or 532 nm (vGmOr2 imaging) laser was shuttered using acousto-optic modulation. For vGpH and GCaMP3 imaging data were acquired at 100 Hz by integrating for 9.74 ms in frame transfer mode and restricting imaging to a sub-area of the CCD chip. Fluo5F imaging data was acquired at 1 kHz (0.974 ms integration time). To estimate 1 AP ΔFs of vGpH, we took the difference between the average 20 frames before and after the stimulus. The rise in vGpH fluorescence in response to a single AP always took two frames when acquiring at 100 Hz time resolution. For display purposes the images in Fig. 1E were given a 2 pixel gaussian average filter. Pv and single AP calcium signals were measured with 4 mM extracellular $CaCl_2$. All stated values are mean±SEM, statistical significance for groups of 3 or more were determined by one-way ANOVA with Tukey's HSD for Post-Hoc analysis. Otherwise Student's t-test was used for determining statistics.

Supplementary Material

Refer to Web version on PubMed Central for supplementary material.

Acknowledgments

We thank Wendy Pratt for performing mutagenesis on $\alpha_2\delta$-1 and Marianna D'Arco for advice on immunocytochemistry. We thank Sunghyun Kim for designing the vGmOr2 and VAMPmCh plasmids, Pablo Ariel for helpful discussion and analysis of exocytosis data, Ricky Kwan and Yogesh Gera for technical assistance in cell culture, Gerald Obermair (Division of Physiology, Innsbruck Medical University) for providing the wild type eGFP-$\alpha 1_A$ plasmid and Loren Looger (Janelia Farms, Howard Hughes Medical Institute) for providing the GCaMP3 plasmid and helpful communication.

References

1. Llinas R, Steinberg IZ, Walton K. Presynaptic calcium currents and their relation to synaptic transmission: voltage clamp study in squid giant synapse and theoretical model for the calcium gate. Proc Natl Acad Sci U S A. 1976; 73:2918–22. [PubMed: 183215]
2. Neher E, Sakaba T. Multiple roles of calcium ions in the regulation of neurotransmitter release. Neuron. 2008; 59:861–72. [PubMed: 18817727]
3. Davies A, et al. The alpha2delta subunits of voltage-gated calcium channels form GPI-anchored proteins, a posttranslational modification essential for function. Proc Natl Acad Sci U S A. 2007; 107:1654–9. [PubMed: 20080692]
4. Field MJ, et al. Identification of the alpha2-delta-1 subunit of voltage-dependent calcium channels as a molecular target for pain mediating the analgesic actions of pregabalin. Proc Natl Acad Sci U S A. 2006; 103:17537–42. [PubMed: 17088553]
5. Wang M, Offord J, Oxender DL, Su TZ. Structural requirement of the calcium-channel subunit alpha2delta for gabapentin binding. Biochem J. 1999; 342 (Pt 2):313–20. [PubMed: 10455017]
6. Neely GG, et al. A genome-wide Drosophila screen for heat nociception identifies alpha2delta3 as an evolutionarily conserved pain gene. Cell. 2010; 143:628–38. [PubMed: 21074052]
7. Gao B, et al. Functional properties of a new voltage-dependent calcium channel alpha(2)delta auxiliary subunit gene (CACNA2D2). J Biol Chem. 2000; 275:12237–42. [PubMed: 10766861]
8. Arikkath J, Campbell KP. Auxiliary subunits: essential components of the voltage-gated calcium channel complex. Curr Opin Neurobiol. 2003; 13:298–307. [PubMed: 12850214]
9. Catterall WA. Structure and regulation of voltage-gated Ca2+ channels. Annu Rev Cell Dev Biol. 2000; 16:521–55. [PubMed: 11031246]
10. Dunlap K, Luebke JI, Turner TJ. Exocytotic Ca2+ channels in mammalian central neurons. Trends Neurosci. 1995; 18:89–98. [PubMed: 7537420]

11. Cao YQ, et al. Presynaptic Ca2+ channels compete for channel type-preferring slots in altered neurotransmission arising from Ca2+ channelopathy. Neuron. 2004; 43:387–400. [PubMed: 15294146]
12. Watschinger K, et al. Functional properties and modulation of extracellular epitope-tagged Ca(V)2.1 voltage-gated calcium channels. Channels (Austin). 2008; 2
13. Winterfield JR, Swartz KJ. A hot spot for the interaction of gating modifier toxins with voltage-dependent ion channels. J Gen Physiol. 2000; 116:637–44. [PubMed: 11055992]
14. Dolphin AC. Calcium channel diversity: multiple roles of calcium channel subunits. Curr Opin Neurobiol. 2009; 19:237–44. [PubMed: 19559597]
15. Pragnell M, et al. Calcium channel beta-subunit binds to a conserved motif in the I–II cytoplasmic linker of the alpha 1-subunit. Nature. 1994; 368:67–70. [PubMed: 7509046]
16. Schneggenburger R, Sakaba T, Neher E. Vesicle pools and short-term synaptic depression: lessons from a large synapse. Trends Neurosci. 2002; 25:206–12. [PubMed: 11998689]
17. Ariel P, Ryan TA. Optical mapping of release properties in synapses. Front Neural Circuits. 2010; 4
18. Catterall WA, Few AP. Calcium channel regulation and presynaptic plasticity. Neuron. 2008; 59:882–901. [PubMed: 18817729]
19. Tian L, et al. Imaging neural activity in worms, flies and mice with improved GCaMP calcium indicators. Nat Methods. 2009; 6:875–81. [PubMed: 19898485]
20. Dodge FA Jr, Rahamimoff R. Co-operative action a calcium ions in transmitter release at the neuromuscular junction. J Physiol. 1967; 193:419–32. [PubMed: 6065887]
21. Parekh AB. Ca2+ microdomains near plasma membrane Ca2+ channels: impact on cell function. J Physiol. 2008; 586:3043–54. [PubMed: 18467365]
22. Canti C, et al. The metal-ion-dependent adhesion site in the Von Willebrand factor-A domain of alpha2delta subunits is key to trafficking voltage-gated Ca2+ channels. Proc Natl Acad Sci U S A. 2005; 102:11230–5. [PubMed: 16061813]
23. Springer TA. Complement and the multifaceted functions of VWA and integrin I domains. Structure. 2006; 14:1611–6. [PubMed: 17098186]
24. Lacy DB, Wigelsworth DJ, Scobie HM, Young JA, Collier RJ. Crystal structure of the von Willebrand factor A domain of human capillary morphogenesis protein 2: an anthrax toxin receptor. Proc Natl Acad Sci U S A. 2004; 101:6367–72. [PubMed: 15079089]
25. Whittaker CA, Hynes RO. Distribution and evolution of von Willebrand/integrin A domains: widely dispersed domains with roles in cell adhesion and elsewhere. Mol Biol Cell. 2002; 13:3369–87. [PubMed: 12388743]
26. Davies A, et al. The calcium channel alpha2delta-2 subunit partitions with CaV2.1 into lipid rafts in cerebellum: implications for localization and function. J Neurosci. 2006; 26:8748–57. [PubMed: 16928863]
27. Brown JT, Randall A. Gabapentin fails to alter P/Q-type Ca2+ channel-mediated synaptic transmission in the hippocampus in vitro. Synapse. 2005; 55:262–9. [PubMed: 15668986]
28. Tran-Van-Minh A, Dolphin AC. The alpha2delta ligand gabapentin inhibits the Rab11-dependent recycling of the calcium channel subunit alpha2delta-2. J Neurosci. 2010; 30:12856–67. [PubMed: 20861389]
29. Kurshan PT, Oztan A, Schwarz TL. Presynaptic alpha2delta-3 is required for synaptic morphogenesis independent of its Ca2+-channel functions. Nat Neurosci. 2009; 12:1415–23. [PubMed: 19820706]
30. Kim SH, Ryan TA. CDK5 serves as a major control point in neurotransmitter release. Neuron. 2010; 67:797–809. [PubMed: 20826311]

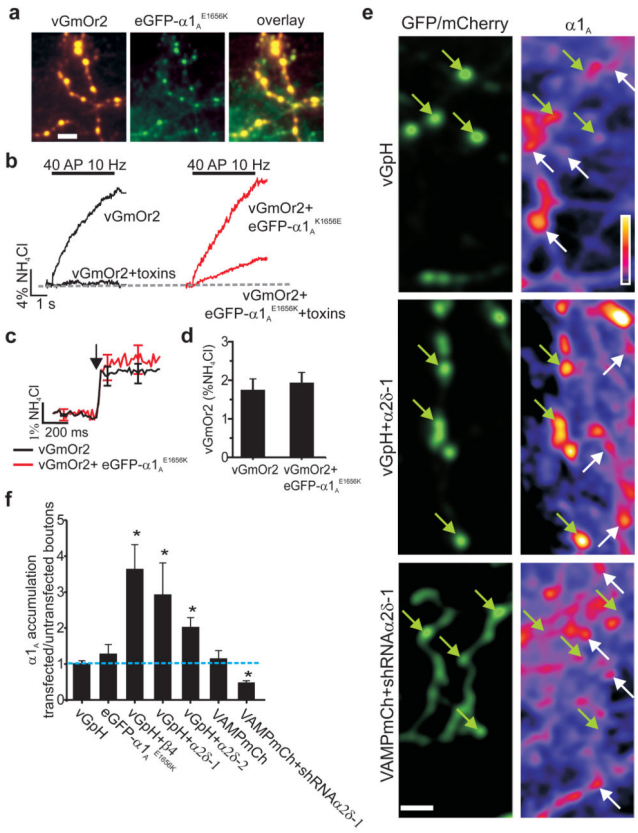

Figure 1. Increased expression of α2δ and β subunits leads to increased P/Q Ca^{2+} channel accumulation at synapses

a, Co-expression of vGmOr2 (left), eGFP–$\alpha1_A^{E1656K}$ (middle), overlay (right). **b**, Exocytic response for vGmOr2 alone (left; n=9) and vGmOr2 coexpressed with eGFP-$\alpha1_A^{E1656K}$ (right; n=6) reveals a significant toxin-resistant response (20±7.1% of pre-toxin). **c**, Average traces of single AP vGmOr2 responses ±eGFP-$\alpha1_A^{E1656K}$ (n>8). Arrow indicates stimulation with 1 AP. **d**, Average ΔF response for data in (**c**) (control 1.76±0.28; n=14; + eGFP–$\alpha1_A^{E1656K}$ 1.91±0.35; n=9; (p>0.1). **e**, Presynaptic $\alpha1_A$ abundance. Green arrows indicate transfected boutons, white arrows indicate non-transfected immunopositive $\alpha1_A$ channel puncta. **f**, ratio of $\alpha1_A$ immunofluorescence intensity in transfected puncta compared to untransfected puncta (n≥8 cells for all conditions). All stated values are mean ±SEM. Inset linear pseudo color LUT scale. Scale bar for all images = 4 μm.

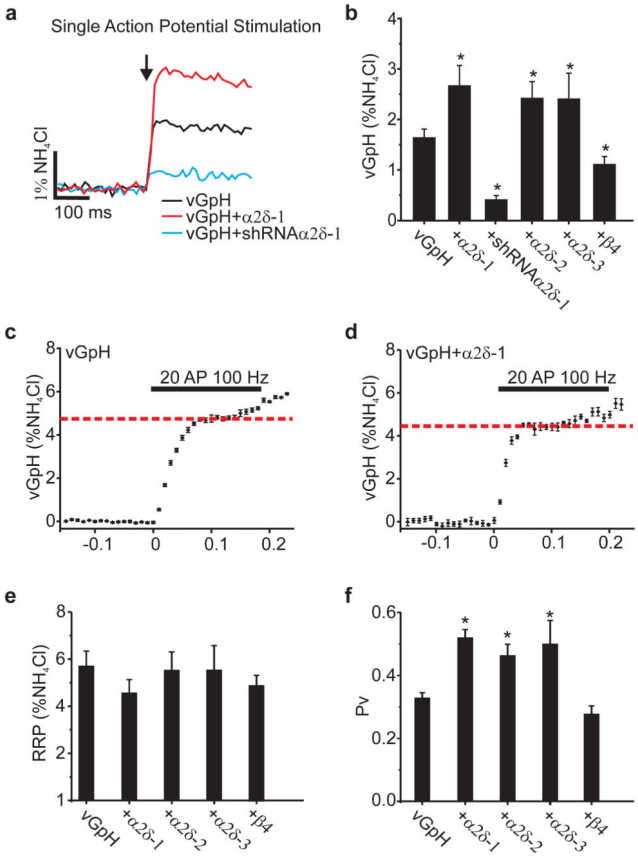

Figure 2. Exocytosis is increased in neurons expressing α2δ

a, Representative single AP vGpH responses (10 trial average, ≈25 boutons). Arrow indicates stimulation with 1 AP. **b**, Summary of single AP response (%NH_4Cl): vGpH= 1.65±0.17; vGpH+α2δ-1= 2.71±0.40; vGpH+α2δ-1shRNA= 0.4±0.08; vGpH+α2δ-2= 2.44±0.36; vGpH+α2δ-3, 2.42±0.51; vGpH+β4= 1.12±0.15, *p<0.01, n≥7. **c–d**, vGpH-based RRP measurements, dotted line identifies RRP. **e**, Summary of RRP size (%NH_4Cl): vGpH= 5.67±0.64, vGpH+α2δ-1= 4.6±0.58, vGpH+α2δ-2= 5.57±0.78, vGpH+α2δ-3= 5.58±1.05, vGpH+β4= 4.92±0.45; (p>0.1; n≥7). **f**, Pv measurements (*p <0.01): vGpH= 0.33±0.02, vGpH+α2δ-1 0.52±0.03, vGpH+α2δ-2= 0.46±0.04, vGpH+α2δ-3= 0.50±0.08, vGpH+β4= 0.28±0.03; n≥7. All stated values are mean±SEM.

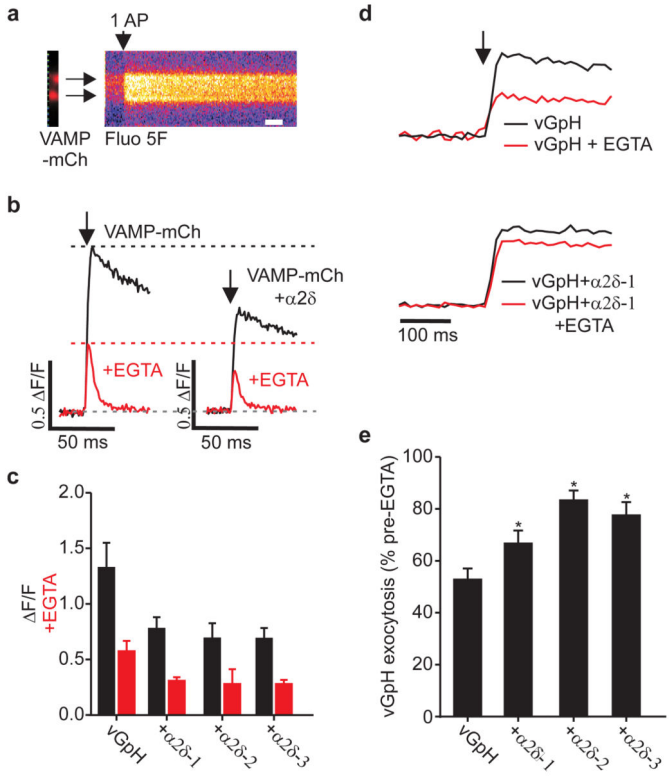

Figure 3. α2δ leads to reduced Ca^{2+} influx and tighter coupling of calcium channels to exocytosis

a, Ca^{2+} influx stimulated by 1 AP (vertical arrow) from boutons identified by VAMP-mCh (left), and visualized by Fluo5F (kymograph, right). Scale bar = 20 ms. **b**, Single traces of Ca^{2+} influx. **c**, Peak Fluo5F signal vs control (*p<0.05): VAMP-mCh 1.3±0.2; +α2δ-1 0.78±0.09; +α2δ-2 0.69±0.13; +α2δ-3 0.69±0.13 (n>8). ΔF/F of Ca^{2+} transient post EGTA (red): VAMP-mCh 0.58±0.09; +α2δ-1 0.32±0.03; +α2δ-2 0.28±0.13; +α2δ-3 0.29±0.03. **d**, Representative traces vGpH±α2δ-2 stimulated by 1 AP (vertical arrow). Traces normalized to response pre-EGTA treatment. **e**, Resistance to EGTA treatment (% exocytosis pretreatment): vGpH 53±4; +α2δ-1 68±6; +α2δ-2 83±4; +α2δ-3 77±5 *p<0.05, n≥7 for all conditions. All stated values are mean±SEM.

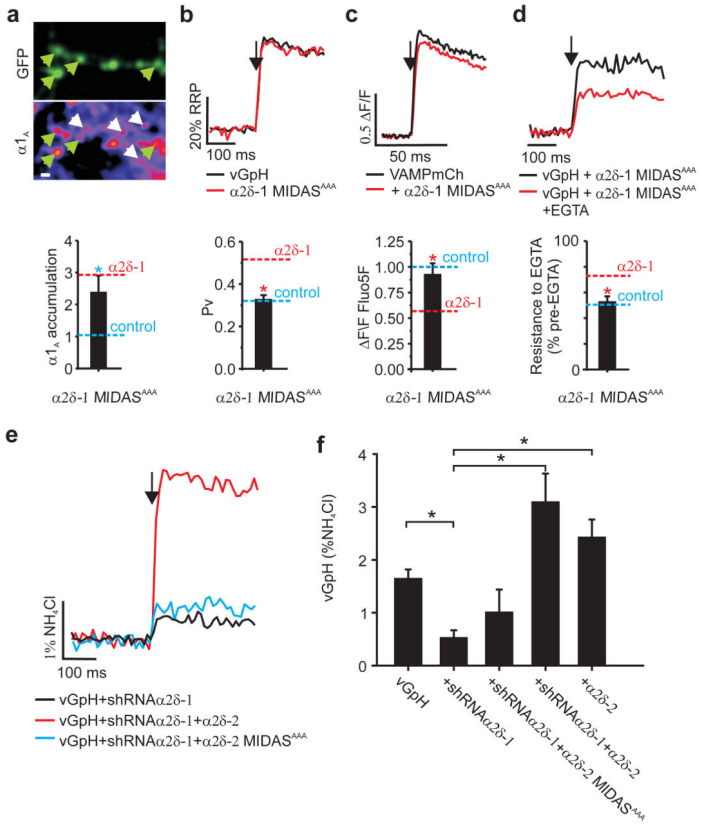

Figure 4. α2δ MIDAS motif is essential for coupling Ca^{2+} channels to exocytosis

a,Top: Presynaptic $\alpha1_A$ abundance. Green arrows indicate transfected boutons, white arrows indicate non-transfected immunopositive $\alpha1_A$ channel puncta.. Scale bar = 2 μm. Bottom: Ratio of $\alpha1_A$ staining in synaptic boutons. Dashed lines represent ratios taken from Fig. 1f as indicated. **b**, Top: Representative vGpH responses to 1 AP (arrow) as a fraction of the measured RRP Bottom: vGpH and α2δ-1 $MIDAS^{AAA}$ (Pv=0.33±0.017) compared to data from Fig. 2f as indicated. **c**, Top: Representative responses to 1 AP-driven Ca^{2+} influx (Fluo5F 3F/F). Bottom: Peak 1 AP Fluo 5F ΔF/F values in cells co-transfected with VAMPmCh (n=11) and α2δ-1 $MIDAS^{AAA}$ (0.88±0.1; n=6) normalized to VAMPmCh alone (*p<0.05). **d**,Top: Representative vGpH response to 1 AP in a neuron co-expressing α2δ-1 $MIDAS^{AAA}$ as indicated. Bottom: Resistance to EGTA block (% block = 51±5, p=0.63) dashed lines compare data from Fig. 3e as indicated. **e**, Representative vGpH responses to 1 AP. **f**, 1 AP response (%NH_4Cl): vGpH=1.65±0.17; vGpH+α2δ-1shRNA=0.4±0.08, v G p H +α2δ-1shRNA+α2δ-2=3.10±.53; vGpH+α2δ-1shRNA+α2δ-2 $MIDAS^{AAA}$=1.02±.41; vGpH+α2δ-2=2.44±0.36. Values are mean±SEM, *p<0.01, n≥7, (*p<0.05).